Metabolic Engineering 76 (2023) 215–224

Contents lists available at ScienceDirect

Metabolic Engineering

journal homepage: www.elsevier.com/locate/meteng

Paving the way for synthetic C1 - Metabolism in *Pseudomonas putida* through the reductive glycine pathway

Lyon Bruinsma [a], Sebastian Wenk [b], Nico J. Claassens [c,**,1], Vitor A.P. Martins dos Santos [a,d,e,*,1]

[a] Laboratory of Systems and Synthetic Biology, Wageningen University & Research, Wageningen, 6708, WE, the Netherlands
[b] Systems and Synthetic Metabolism Group, Max Planck Institute of Molecular Plant Physiology, Potsdam-Golm, Germany
[c] Laboratory of Microbiology, Wageningen University & Research, Wageningen, 6708, WE, the Netherlands
[d] LifeGlimmer GmbH, Berlin, 12163, Germany
[e] Bioprocess Engineering, Wageningen University & Research, Wageningen, 6708, WE, the Netherlands

ARTICLE INFO

Keywords:
One-carbon metabolism
Carbon fixation
Metabolic engineering
Synthetic biology
Sustainable biotechnology
Pseudomonas putida

ABSTRACT

One-carbon (C1) compounds such as methanol, formate, and CO_2 are alternative, sustainable microbial feedstocks for the biobased production of chemicals and fuels. In this study, we engineered the carbon metabolism of the industrially important bacterium *Pseudomonas putida* to modularly assimilate these three substrates through the reductive glycine pathway. First, we demonstrated the functionality of the C1-assimilation module by coupling the growth of auxotrophic strains to formate assimilation. Next, we extended the module in the auxotrophic strains from formate to methanol-dependent growth using both NAD and PQQ-dependent methanol dehydrogenases. Finally, we demonstrated, for the first time, engineered CO_2-dependent formation of part of the biomass through CO_2 reduction to formate by the native formate dehydrogenase, which required short-term evolution to rebalance the cellular NADH/NAD $^+$ ratio. This research paves the way to further engineer *P. putida* towards full growth on formate, methanol, and CO_2 as sole feedstocks, thereby substantially expanding its potential as a sustainable and versatile cell factory.

1. Introduction

Current biotechnological production of chemicals and fuels primarily depends on sugars and other plant biomass fractions as substrates. However, there are serious sustainability concerns related to these substrates due to their competition for land with biodiversity and food production (Wendisch et al., 2016). Therefore, alternative microbial feedstocks need to be urgently considered. One-carbon (C1) feedstocks are considered prime sustainable alternatives, as CO_2 or reduced C1-feedstocks can be obtained from abundantly available atmospheric CO_2 or waste gas streams. CO_2 can be converted into chemicals and fuels by microorganisms when supplied with an inorganic energy source or a reduced C1-source. Chemical (electro)catalytic methods are increasingly being developed to efficiently convert CO_2 into the soluble, reduced C1-molecules formate and methanol (Fan et al., 2020; Liu et al., 2020). The production of e-methanol from CO_2 and electricity is already being scaled at an industrial scale in Iceland (Cotton et al., 2020; Stöckl et al., 2022). Both methanol and formate were identified as promising microbial feedstocks, given their liquid nature, and are therefore relatively easy to feed into the bioproduction process compared to the gaseous C1-molecules (Claassens et al., 2018; Cotton et al., 2020; Naik et al., 2010; Wendisch et al., 2016).

Energy-efficient conversion of C1-substrates into products can be achieved by anaerobic acetogenic bacteria. The bioproduction of ethanol from syngas (H_2, CO, and CO_2) has already been realized industrially, and the anaerobic production of some other products has been demonstrated (Köpke and Simpson, 2020; Liew et al., 2022). However, these strictly anaerobic acetogens are relatively hard to modify genetically and can only generate a limited product spectrum due to their low availability of ATP (Bertsch and Müller, 2015).

Alternatively, the aerobic conversion of C1-substrates could be harnessed for a wider product spectrum, yet many aerobic C1-utilizers use energy-inefficient assimilation pathways and/or are hard to genetically modify (Claassens et al., 2019; Whitaker et al., 2015). Attractive aerobic

* Corresponding author. Laboratory of Systems and Synthetic Biology, Wageningen University & Research, Wageningen, 6708, WE, the Netherlands.
** Corresponding author.
E-mail addresses: nico.claassens@wur.nl (N.J. Claassens), vitor.martinsdossantos@wur.nl (V.A.P. Martins dos Santos).
[1] Contributed equally.

https://doi.org/10.1016/j.ymben.2023.02.004
Received 26 September 2022; Received in revised form 10 February 2023; Accepted 10 February 2023
Available online 15 February 2023

biotechnological production organisms, such as *Escherichia coli, Saccharomyces cerevisiae,* and *Pseudomonas putida* are naturally unable to grow on C1-substrates. Nevertheless, in recent years efforts have been made in the former two organisms to establish synthetic methanol and formate assimilation. Especially efforts in *E. coli* have been successful, in which full synthetic methylotrophy and formatotrophy have been established (Chen et al., 2020; Keller et al., 2022; Kim et al., 2020). However, the growth rates and yields of these *E. coli* strains on methanol and formate are not sufficient yet for industrial performance.

As an alternative bioproduction host, *P. putida* has emerged in recent years, as this soil bacterium is naturally endowed to withstand harsh conditions and physiochemical stresses. These features make it an industrially relevant microbe for which the generation of a plethora of products has been demonstrated (Ankenbauer et al., 2020; Martin--Pascual et al., 2021; Nikel and de Lorenzo, 2018; Poblete-Castro et al., 2012). *P. putida* cannot naturally grow on C1-substrates, and so far only the use of formate as an auxiliary energy source and the partial establishment of the Ribulose Monophosphate Pathway (RuMP) has been demonstrated (Koopman et al., 2009; Zobel et al., 2017). The RuMP can allow for efficient growth on methanol, but this pathway does not allow for growth on formate or CO_2. Hence, to realize sustainable bioproduction using diverse C1-substrates in *P. putida*, efficient assimilation pathways must be established.

Several pathways can be considered to establish C1-assimilation in this bacterium. Typical natural pathways for C1-assimilation such as the Calvin Cycle, RuMP, and Serine Cycle can allow for growth on CO_2, methanol, and/or formate (Antoniewicz, 2019; H. Yu and Liao, 2018). However, all share the disadvantage of having a cyclic architecture in which a pathway metabolite needs to be regenerated for assimilation. Moreover, they have an intensive overlap.

with the host's native metabolism, making their engineering more challenging (Bar-Even et al., 2013; Barenholz et al., 2017; Chen et al., 2020; Gleizer et al., 2019; Keller et al., 2022). Additionally, the Calvin Cycle and the Serine Cycle are relatively energy-inefficient due to their high ATP consumption. In recent years, the reductive glycine pathway (rGlyP) has been suggested as an alternative pathway for C1-assimilation in model microbes. This linear pathway was first designed as a synthetic pathway and recently found in nature as a CO_2 and formate assimilation pathway (Bar-Even et al., 2013; Cotton et al., 2018; Figueroa et al., 2018; Löwe and Kremling, 2021; Sánchez-Andrea et al., 2020).

In the rGlyP, formate is converted to 5,10-methylene-THF through consecutive THF-ligation and reduction reactions. Next, 5,10-methylene-THF, together with CO_2, ammonia, and NADH produces glycine in the glycine cleavage system (GCS), which can operate in the reverse direction under elevated CO_2 concentrations. Then, glycine can be condensed with a second molecule of 5,10-methylene-THF to produce serine (Fig. 1).

At last, serine can be converted to pyruvate through deamination and from thereon to biomass (Bar-Even et al., 2013; Claassens et al., 2022; Yishai et al., 2017; 2018). This formate assimilation pathway can be further extended towards methanol assimilation by adding a module containing a methanol and a formaldehyde dehydrogenase. Moreover, when equipped with a CO_2-reducing formate dehydrogenase (FDH) and an additional energy source, the rGlyP could allow full growth on CO_2 as the sole substrate (Fig. 1).

Modular implementation of the rGlyP has recently led to the full establishment of this pathway in *E. coli* for growth on formate and methanol, and in *Cupriavidus necator* for growth on formate (Kim et al., 2020; Claassens et al., 2020). Another recent work has demonstrated the establishment of the core of the rGlyP in *S. cerevisiae*, by converting formate into glycine (Gonzalez De La Cruz et al., 2019). The assimilation of CO_2 into the rGlyP has been proposed before, but it has not yet been demonstrated experimentally in an engineered strain (Cotton et al., 2018).

The rGlyP is due to its high ATP-efficiency the aerobic pathway that

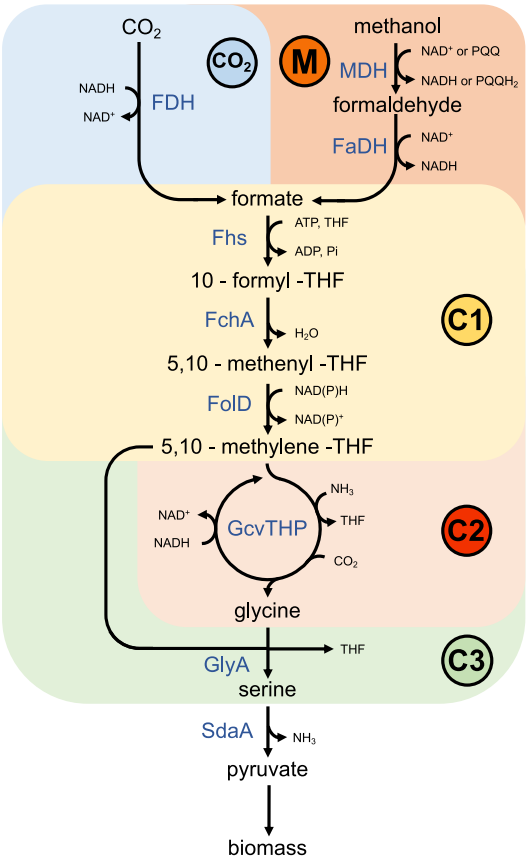

Fig. 1. Core module of the reductive glycine pathway implemented in this study. The pathway is divided into several modules. The CO_2 and M modules convert CO_2 and methanol to formate, respectively. Formate is then converted to 5,10-methylene-THF in the C1 module. Subsequently, the 5,10-methylene-THF is converted to glycine by the C2 module comprising the reverse glycine cleavage system. In the C3 module, glycine is condensed with 5,10-methylene-THF to produce serine. Then, serine is deaminated to pyruvate which provides the cell with the needed biomass. Abbreviations: (FDH), formate dehydrogenase, (MDH), methanol dehydrogenase, (FaDH), formaldehyde dehydrogenase, (Fhs), formate THF-ligase, (FchA), formyltetrahydrofolate cyclohydrolase (FolD), bifunctional methylenetetrahydrofolate dehydrogenase/methyltetrahydrofolate cyclohydrolase, (GcvTHP), glycine cleavage system, (GlyA), serine hydroxymethyltransferase, (SdaA), serine deaminase, (THF), tetrahydrofolate.

can provide the highest theoretical yield on formate (Bar-Even et al., 2013; Cotton et al., 2020; Löwe and Kremling, 2021). Also, for growth on CO_2 as the sole carbon source, the rGlyP is the most ATP-efficient aerobic pathway known; though there is an energetic disadvantage of this pathway due to the thermodynamics of the CO_2 to formate reduction reaction and its dependence on elevated CO_2. However, high-concentration CO_2 streams are commonly available and applied as a feed in industrial biotechnology (Cotton et al., 2018; Löwe and Kremling, 2021) For growth on methanol, the rGlyP is energetically only rivaled by the RuMP. Yet, the rGlyP can support higher yields than the RuMP for more oxidized products (e.g. pyruvate or lactate) as the rGlyP supports co-fixation of CO_2 with the highly reduced substrate methanol (Cotton et al., 2020; Löwe and Kremling, 2021).

In this study, we establish the foundation for C1-assimilation by complementing biomass through the rGlyP for formate, methanol, and CO_2 in *P. putida*. We follow a growth-coupled modular engineering approach using specific auxotrophic strains to establish the core of the rGlyP (Orsi et al., 2021). We demonstrate the assimilation of formate, as well as methanol, through the core of the rGlyP into serine. Moreover, we demonstrate, for the first time, a growth-coupled selection for CO_2

fixation through reverse FDH activity into the rGlyP. Overall, this work demonstrates C1-assimilation of three highly promising C1-feedstocks in *P. putida*. The eventual establishment of complete C1-metabolism will substantially strengthen the position of *P. putida* as an industrial chassis in the bio-industry and thereby contribute to the transition to a biobased economy.

2. Results

2.1. Implementing the reductive glycine pathway

To implement the rGlyP, we split the pathway into three modules: C1, C2, and C3 (Fig. 1). The C1 module converts formate to 5,10-methylene-THF, which is further converted to glycine via the reverse operation of the GCS in the C2 module. In the C3 module, glycine is condensed with another 5,10-methylene-THF to serine. Finally, serine can be converted to pyruvate and from there to biomass.

We constructed two auxotrophic strains in which the functionality of the modules could be coupled to growth, i.e., if the modules are functional the auxotrophy is relieved and the strains will grow. To test the C1 and C3 modules, we constructed a growth-coupled design termed C1–S-Aux by deleting the genes of both GCSs (Δ*gcvTPH-I /II*) and the D-3-phosphoglycerate dehydrogenases (Δ*serA* /ΔPP_2533) (Fig. 2A). This strain is unable to produce serine and the C1-precursor molecules (e.g. 5,10-methylene-THF), which are essential for the biosynthesis of purines, thymidine, coenzyme A and methionine (Yishai et al., 2017). In this strain, growth on a canonical carbon source (e.g., glucose) can only be restored when serine is supplemented, or when both C1 and C3 modules are present and active with glycine and formate as substrates. In this case, the C1 module will convert formate into 5,10-methylene-THF, and the C3 module will condense 5,10-methylene-THF with glycine to form serine (Fig. 2a). To realize the heterologous expression of

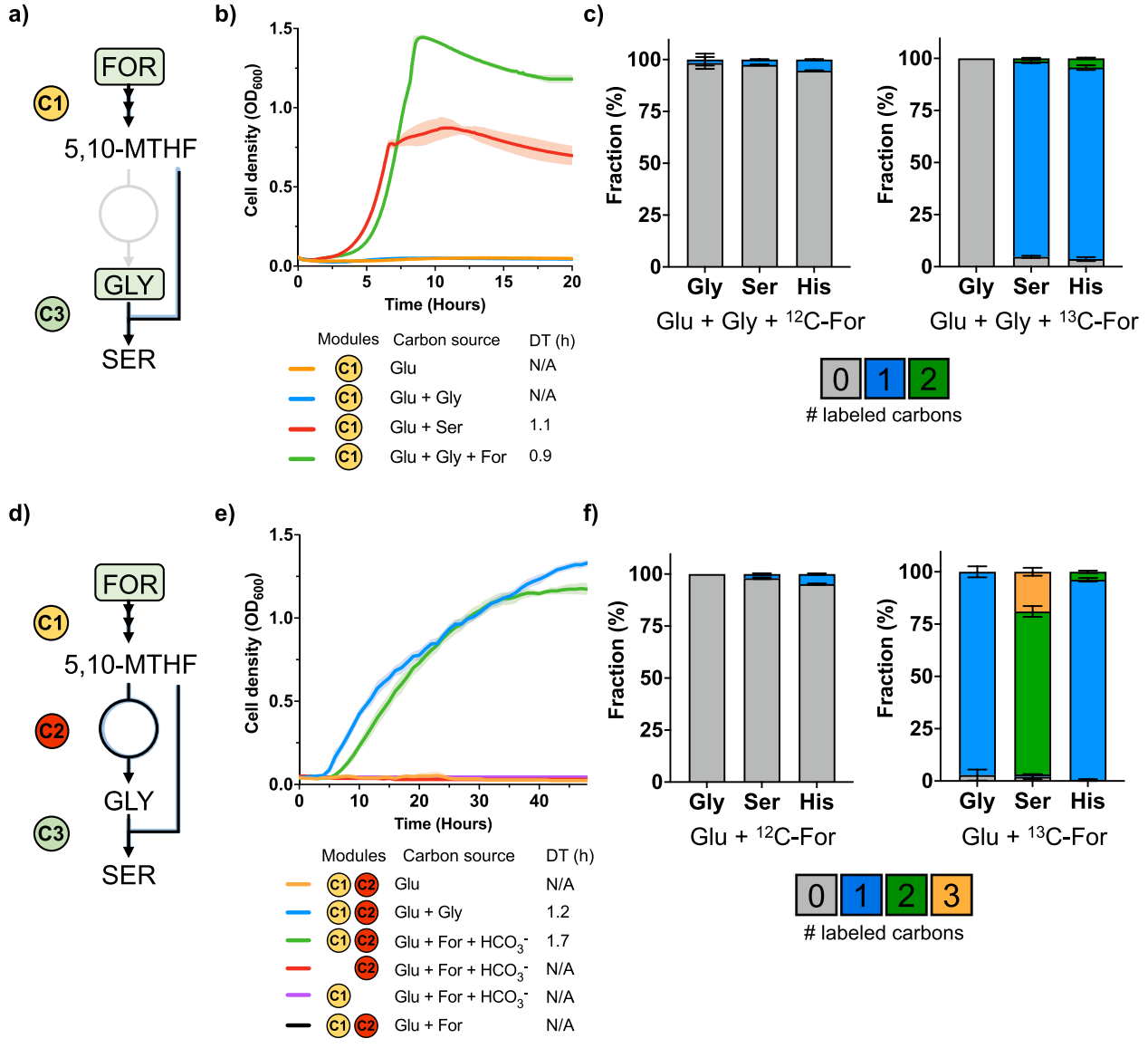

Fig. 2. Formate-dependent growth. a) Selection of the C1 and C3 module in C1–S-aux. Growth is only possible when serine is supplemented to the medium or if both glycine and formate are present. **b)** Growth of C1–S-aux. Overexpression of the C1 module converts formate to replenish the cellular C1-moieties. The C3 module subsequently produces serine, restoring growth. **c)** ^{13}C labeling experiments confirm that cellular C1-moieties are produced from formate. **d)** Selection of the combined activity of the C1, C2, and C3 modules in C1-G-S-Aux. **e)** Growth of C1-G-S-Aux. Growth can solely be restored when glycine or formate are added to the medium (at elevated CO_2 levels through the addition of 100 mM sodium bicarbonate). **f)** ^{13}C labeling experiments confirm that cellular C1-moieties, glycine, and serine are produced from formate and CO_2. Abbreviations: (Gly), glycine, (Ser), serine, (His), histidine, (For), formate, (5,10-MTHF), 5,10-methylene-THF, (Glu), glucose, (HCO_3^-), bicarbonate, (N/A), not applicable. Growth curves and labeling experiments represent the mean value ± SD from three biological replicates.

the C1 module, we created the pC1 plasmid by introducing the formate-THF ligase (*fhs*), 5,10-methenyl-THF cyclohydrolase (*fchA*), and the bifunctional 5,10-methenyl-THF cyclohydrolase /5,10-methylene-THF dehydrogenase (*folD*) genes from *Clostridium ljunghdahlii* DSM13528 on a SEVAb24 backbone. We equipped the C1–S-Aux strain with pC1 and tested the growth of the strain on a medium containing glucose, glycine, and formate. We observed that the C1 and C3 module could carry enough flux into the C1-pool and serine to restore growth of C1–S-Aux. Growth occurred at a similar growth rate (doubling time ~1 h) and even a higher biomass yield than for the control medium with glucose and serine (Fig. 2b). Overexpression of the C3 module was not necessary as endogenous activity was enough to restore growth. When formate was omitted from the medium, no growth was observed, which reflects its dependency on the assimilation of formate via the C1 module of the rGlyP. To confirm this dependency, we performed labeling experiments with ^{13}C-labeled formate and measured the labeling in the proteinogenic amino acids glycine, serine, and histidine (Fig. 2c). If the C1 and C3 modules are functioning as expected, serine is derived from the condensation of unlabeled glycine with once-labeled 5,10-methylene-THF (derived from ^{13}C-formate). Histidine biosynthesis requires the incorporation of 10-formyl-THF, coming from formate in the C1 module, so it should also be labeled once. As expected, both serine and histidine were almost completely labeled once, confirming the activity of the C1 and C3 modules.

Next, we aimed to test the C2 module, which comprises the reverse operation of the GCS. To test this module, we built a growth-coupled selection strain termed C1-G-S-Aux by deleting the genes encoding threonine aldolase (Δ*ltaE*), and isocitrate lyase (Δ*aceA*), as well as *serA* and PP_2533. This strain is unable to produce serine, glycine, and the C1-precursor molecules and requires external supplementation of serine or glycine for growth on glucose (Yishai et al., 2018). By the combined activity of the C1, C2, and C3 modules, formate together with CO_2 can generate glycine and subsequently serine to relieve the auxotrophy (Fig. 2d). The GCS can run in the reverse direction at elevated CO_2 levels, which we created by supplementing the media with 100 mM sodium bicarbonate. It is unclear if the GCS uses CO_2 or bicarbonate, but these carbon species can be interconverted intracellularly by the native carbonic anhydrase (PP_0100). As the native expression level of the GCS is likely not high enough to sustain enough flux, we designed a plasmid to overexpress the native GCS system. We constructed plasmid pC2 (SEVAb65 backbone) overexpressing the endogenous *gcvT-I*, *gcvP-I,* and *gcvH-I* genes. We transformed C1-G-S-Aux with the plasmids pC1 and pC2 and were able to restore growth upon the addition of formate, at a slightly lower growth rate (doubling time 1.7 h) and yield than for the glycine-supplemented control. (Fig. 2e). No growth was observed when both modules were present and no bicarbonate was supplied, indicating that growth is not possible without elevated CO_2 levels. Similar to C1–S-Aux, the endogenous activity of the C3 module was sufficient to restore growth. Isotopic labeling of the proteinogenic amino acids glycine, serine, and histidine after growth on ^{13}C-formate further confirmed the combined activity of the rGlyP modules (Fig. 2f). Glycine is produced by the condensation of labeled 5,10-methylene-THF and unlabeled CO_2 in the GCS and is expected to be labeled once. Almost all the glycine was labeled once, confirming the combined activity of the C1 and C2 modules. Serine is expected to be labeled twice as it is produced from once-labeled glycine plus a labeled 5,10-methylene-THF molecule. As expected, serine was predominantly labeled twice.

2.2. Extending the reductive glycine pathway with methanol assimilation

After demonstrating formate assimilation via the C1, C2, and C3 modules of the rGlyP we wanted to test if these modules could also serve to support methanol assimilation in *P. putida* (Fig. 1). Like formate, methanol is a soluble microbial feedstock that can be efficiently generated from CO_2 and renewable electricity (Szima and Cormos, 2018). Methanol is converted to formate in two enzymatic steps. First, methanol is oxidized to formaldehyde by a methanol dehydrogenase (MDH). Second, formaldehyde is further oxidized to formate by a formaldehyde dehydrogenase. From here on formate can be further assimilated through the engineered modules described before. To engineer methanol utilization in *P. putida,* we constructed the M module comprising the necessary enzymes to oxidize methanol to formate. The genome of *P. putida* encodes for more than 20 alcohol dehydrogenases, yet none of them is annotated as an MDH. However, it was previously reported that some innate alcohol dehydrogenases could have a side activity towards methanol (Koopman et al., 2009). The first candidate is a pyrroloquinoline quinone (PQQ) dependent alcohol dehydrogenase, encoded by *pedE*, that showed activity towards methanol as a substrate (Wehrmann et al., 2017). The second candidate is a native alcohol dehydrogenase, encoded by *adhP*. Through BLAST analyses, we found that the *adhP* gene encodes a homolog of the MDH of *C. glutamicum* (identity: 41.5%). Apart from these two candidates, we tested native or engineered enzymes originating from various organisms that were previously described to catalyze NAD-dependent methanol oxidation: *Bacillus methanolicus, Geobacillus stearothermophilus, Corynebacterium glutamicum,* and *Cupriavidus necator* (Wenk et al., 2020; Wu et al., 2016). For the oxidation of formaldehyde to formate, we overexpressed the *fdhA* gene of *P. putida*, encoding a NAD-dependent formaldehyde dehydrogenase. The various MDH candidate genes and *fdhA* were cloned into pC1, creating pM. We transformed C1–S-Aux with the various pM plasmids to assess which MDH candidate can sustain the highest flux and therefore growth. Without the plasmid expression of an MDH (M-module) no growth was observed. All MDH candidates were able to restore growth of the C1–S-Aux strain on glucose, glycine, and methanol, albeit with different growth patterns (Fig. S1). The engineered MDH from *C. necator* was able to sustain the best growth (10 h doubling time) with the shortest lag phase (Fig. 3b). Next, growth was fastest restored using the MDH from *B. methanolicus* and *C. glutamicum*, followed by *adhP* and *G. stearothermophilus.* The PQQ-dependent alcohol dehydrogenase from *P. putida* was able to sustain growth (11 h doubling time) despite its long lag phase compared to the strains expressing a NAD-MDH. As far as we know, this is the first time an overexpressed PQQ-dependent enzyme has been demonstrated for engineered methanol oxidation. Methanol oxidation using PQQ instead of NAD^+ as an electron acceptor can be potentially advantageous as it has a larger thermodynamic driving force, −35.2 kJ/mol compared to 30.5 kJ/mol ($\Delta_rG'^m$, pH 7.5, ionic strength 0.25 M) (Cotton et al., 2020; Whitaker et al., 2015). NAD-MDH activity is notorious for being a thermodynamic, as well as a kinetic bottleneck for synthetic methylotrophy (Woolston et al., 2018). Even though we showed proof of principle for the PQQ-dependent operation of an MDH, the best NAD-MDH results in faster growth in C1–S-Aux. Still, further optimization of PQQ-MDHs, including for example upregulation of native *P. putida* PQQ biosynthesis, can possibly sustain faster growth rates and may be beneficial to support full methylotrophy. However, in this work, we further proceeded with the best-performing NAD-MDH from *C. necator* to demonstrate the potential of the rGlyP for synthetic methylotrophy in *P. putida* (Fig. 3b).

Just as with formate, methanol became essential for the growth of C1–S-Aux, and omitting it from the medium resulted in no growth. Labeling experiments with ^{13}C-methanol further confirmed the combined activity of the M, C1, and C3 modules. As expected, serine and histidine were both labeled once (Fig. 3c).

We further tested methanol assimilation via the rGlyP till serine in the C1-G-S-Aux strain. Hereto, we tested pM with the engineered MDH from *C. necator* together with pC2. Experiments were performed at elevated CO_2 to reverse the GCS reaction by supplying 100 mM sodium bicarbonate to the medium. Through the combined effort of the M, C1, C2, and C3 modules, methanol together with CO_2 could potentially provide the cell with the necessary glycine and serine. As expected, growth was restored upon expression of all the modules and the addition of the required C1-compounds (Fig. 3e). We performed labeling experiments to confirm the activity of the combined modules (Fig. 3f). We

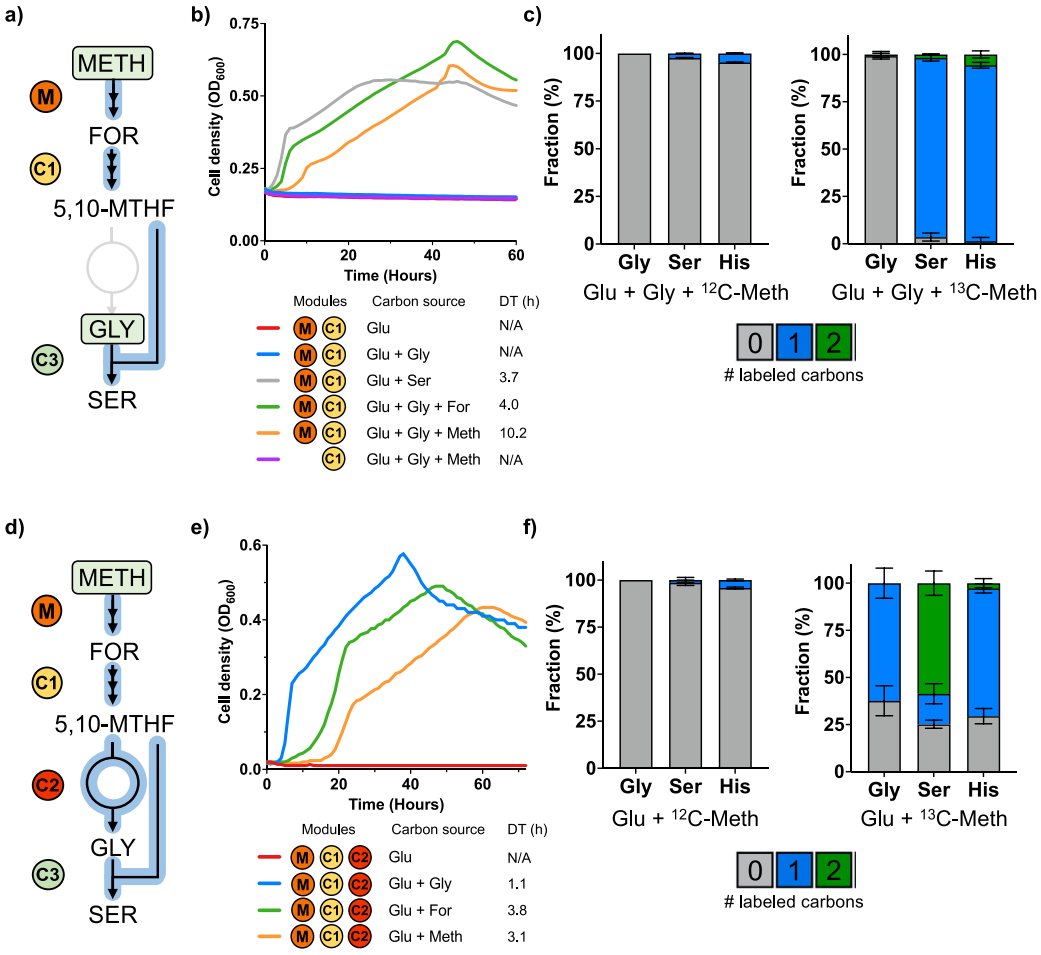

Fig. 3. Methanol-dependent growth. a) Selection of the M, C, and C3 modules in C1–S-Aux. Growth is only possible when serine is supplemented to the medium or if both glycine and formate or methanol are present. **b)** Growth of C1–S-Aux expressing the MDH CT4-1 from *Cupriavidus necator*. Growth is only possible upon overexpression of the M and C1 module, which replenishes the cellular C1-precursor molecules. **c)** ^{13}C labeling experiments confirm that cellular C1-moieties are produced exclusively from methanol **d)** Selection of the combined effort of the M, C1, C2, and C3 modules in C1-G-S-Aux **e)** Growth of C1-G-S-Aux. Growth can solely be restored when glycine or methanol or formate are added to the medium (at elevated CO_2 levels through the addition of 100 mM sodium bicarbonate) **f)** ^{13}C labeling experiments confirm that cellular C1-moieties, glycine, and serine are produced mostly from methanol and CO_2. Abbreviations: (Gly) glycine, (Ser), serine, (His), histidine, (Meth), methanol, (For), formate (5,10-MTHF), 5,10-methylene-THF, (Glu), glucose, (N/A), not applicable. Growth curves and labeling experiments represent the mean value ± SD from three biological replicates.

note that a small fraction of all glycine and serine is unlabeled. Glycine can be produced by the amination of glyoxylate through promiscuous aminotransferase enzymes. However, the isocitrate lyase (*aceA*) is deleted in C1-G-S-Aux, making it unable to produce glyoxylate. We hypothesize that a latent unidentified reaction in *P. putida* can still produce glycine, e.g., from threonine, and was activated during growth of C1-G-S-Aux on methanol, contributing to the unlabeled fraction (~37% of glycine). Nonetheless, taking the growth and labeling patterns into account, we can still conclude that methanol assimilation via the modules of the rGlyP carries most of the flux in C1-G-S-Aux.

2.3. Extending the reductive glycine pathway with CO_2 fixation

Apart from methanol oxidation, formate can be produced through CO_2 reduction (Calzadiaz-Ramirez and Meyer, 2022; Choe et al., 2014; Ragsdale and Wood, 1991; Reda et al., 2008; Sánchez-Andrea et al., 2020; X. Yu et al., 2017). FDHs commonly convert formate to CO_2, which is thermodynamically the most favorable direction. However, metal-dependent FDHs, using molybdenum or tungsten, can also serve in CO_2 fixation pathways by reducing CO_2 to formate (Cotton et al., 2018; Maia et al., 2017). The genome of *P. putida* accounts for two native FDHs. The genes *fdoGHI-fdhE* (PP_0489–0492) encode a membrane-bound FDH, which possibly uses quinol as a redox cofactor. The second FDH (PP_2183–2186) is a soluble NAD-dependent molybdenum-containing FDH (Zobel et al., 2017). We reasoned that the molybdenum-containing NAD-FDH from *P. putida* could be able to reduce CO_2 to formate and serve as an entry point for the rGlyP. To test this hypothesis, we constructed pCO_2 containing PP_2183–2186 on a SEVA83b backbone.

We transformed C1–S-Aux with both pC1 and pCO_2 and grew the strain in sealed bottles containing 20 mM glucose, 10 mM glycine, and CO_2. The thermodynamics of CO_2 reduction are highly unfavorable ($\Delta_rG'^m = 14.4$ kJ/mol, pH 7.5, ionic strength 0.25 M) (Flamholz et al., 2012). Therefore, we filled the headspace of the bottles with 50% (v/v) CO_2 to push the reduction reaction. After a few weeks of incubation, we observed growth in one of the bottles. Reinoculation of this strain in fresh media with glucose, glycine, and 50% CO_2 enabled immediate growth (Fig. S2b). We cultivated this strain, termed C1–S-Evo, in a range of different CO_2 concentrations, from ambient (0.04%) to 50%, to examine the CO_2 dependency of this strain. We observed that growth was highly dependent on the concentration of CO_2 added to the headspace (Fig. 4b). Fast growth was observed when the headspace was filled with 20–50% CO_2, with doubling times ranging from 13.7 down to 6.0 h, respectively. Growth still occurred at 10% CO_2, albeit with a lower

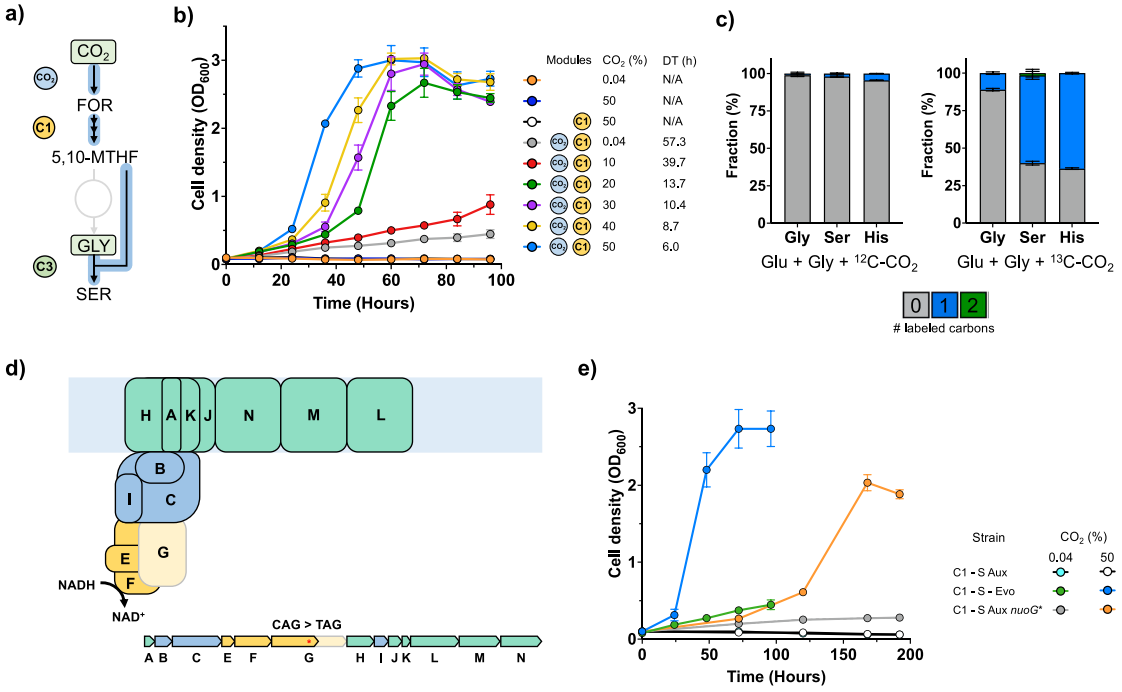

Fig. 4. CO_2-dependent growth. A) Selection of the CO_2, C1, and C3 modules in C1–S-Aux/Evo. Growth is only possible when serine is supplemented to the medium or if both glycine and CO_2 are present. **B)** Growth of C1–S-Evo in different CO_2 concentrations. Growth is only possible upon overexpression of the CO_2 and C1 module, which replenishes the cellular C1-moieties. Growth is heavily dependent on the increasing CO_2 concentrations. **C)** ^{13}C labeling experiments confirm that cellular C1-moieties are produced mostly from CO_2. Data is derived from cells growing at 50% (v/v) CO_2. **D)** Localization of the NuoG protein within complex I of the electron transport chain. The acquired stop codon (CAG > TAG) during evolution allows translation of only half the NuoG protein. Figure adapted from (Chadwick et al., 2018). **E)** Retro engineering of the TAG stop codon in the *nuoG* gene in C1–S-Aux. Growth was restored due to this single mutation at ambient (0.04) and 50% (v/v) CO_2 by expressing the C1 and mutated CO_2 module. Abbreviations: (Gly) glycine, (Ser), serine, (His), histidine, (For), formate, (5,10-MTHF), 5,10-methylene-THF, (Glu), Glucose, (N/A), not applicable. Growth curves and labeling experiments represent the mean value ± SD from three biological replicates.

doubling time (39.7 h). The clear dependency of the growth phenotype on the CO_2 concentration is likely related to the thermodynamic driving force of CO_2 reduction by FDH, which can be improved by increasing CO_2 concentrations. Growth was not observed when the pCO_2 plasmid was omitted, indicating that growth relies on the overexpression of FDH. Moreover, we noticed that this strain was able to grow at ambient CO_2 levels (Fig. 4b, gray line). We hypothesized that the respiration of glucose (still proceeding to supply other biomass components than C1) increases the CO_2 concentration in the headspace, driving formate biosynthesis. To test this hypothesis, we cultivated the strain in a closed and open environment, wherein the latter the CO_2 can freely escape. In both instances, growth occurred similarly (Fig. S3b). This indicates that the CO_2 present in the air and/or intracellularly generated from glucose respiration is enough to drive the reverse reaction toward formate production.

To elucidate what changes had occurred during evolution to allow these CO_2-fixing phenotypes, the pC1 and pCO_2 plasmids of three growing isolates were sequenced.

We discovered a point mutation in the −35 box of the promoter of the CO_2 module, lowering its expression by 31.5-fold based on GFP fluorescence, indicating that the initial expression level of the promoter was too high (Fig. S4). We transformed C1–S-Aux with pC1 and the mutated pCO_2 plasmid, to analyze if this mutation was the sole cause for growth. However, no immediate growth was observed (Data not shown). Therefore, genomic alterations likely contributed to establish this CO_2-dependent growth phenotype. We sequenced the genomes of three purified colonies from the evolved population and discovered four common mutations in all three isolates (Table S4). The most noticeable mutation was the introduction of a stop codon in the middle of the *nuoG* gene encoding the G subunit of the NADH-quinone oxidoreductase (complex I) in the electron transport chain. This complex is directly responsible for NADH oxidation and is needed to regenerate NAD^+ for glycolysis. The occurred mutation allows translation of only half of *nuoG*, probably either interrupting or decreasing the NADH oxidation activity complex I (Fig. 4d). *P. putida* is an obligate aerobic bacteria, which relies on constitutive NADH dehydrogenase activity to oxidize NADH to NAD^+ (Nies et al., 2020). This innate high NADH oxidation activity competes with FDH over NADH availability, likely preventing CO_2 reduction in the unevolved strain. Thus, we hypothesize that this mutation causes a redox perturbance that increases NADH levels for CO_2 reduction.

We reverse-engineered the stop codon mutation in *nuoG* in C1–S-Aux to test the influence of this mutation and transformed the strain with pC1 and the mutated pCO_2 plasmid. After the introduction of this mutation, growth could occur at ambient and 50% CO_2 without the need for evolution, showcasing the beneficial effect of this mutation (Fig. 4e). However, growth was still lagging compared to the evolved strain, so some of the other mutations may have contributed partly to the phenotype.

To further prove CO_2 reduction and its entry into the rGlyP, we performed labeling experiments with ^{13}C–CO_2 (Fig. 4c). Here, serine was expected to be completely labeled once, but only ~60% was once labeled. As glycine was labeled for ~10%, this indicates that at least 50% of the labeled serine originates from labeled 5,10-methylene-THF. We demonstrated earlier that CO_2 released from glucose respiration is enough to drive the reverse FDH reaction resulting in slow growth (Fig. S3b). Therefore, it is likely that a mixture of labeled, as well as unlabeled intracellular CO_2 originating from glucose, is being fixed by the FDH, leading to mixed labeling patterns. This pattern is repeated for histidine, which should theoretically be fully labeled once. To estimate the intracellular labeling status of CO_2, we analyzed the proteinogenic amino acids proline and arginine (Fig. S5). In the biosynthesis of

arginine, one CO_2 is added through carboxylation, which is not present in proline. All other carbons of proline and arginine have the same origin (Gleizer et al., 2019). Therefore, the difference in labeling between these two amino acids can be used to estimate the labeling of intracellular CO_2. This analysis showed that ~76% of intracellular CO_2 is labeled. This explains part of the unlabeled serine and histidine, but one would expect somewhat higher labeling than 60% for serine. This may indicate some uncertainty in the method to determine intracellular CO_2 or some (small) contribution of other latent pathways to C1-biosynthesis other than CO_2 reduction. However, considering the dependency of growth on CO_2 and labeling patterns (~50–60% for serine and histidine), we can conclude that CO_2 fixation via the reverse FDH reaction is the main contributor to C1-biosynthesis.

After establishing CO_2-dependent growth in the C1–S-Evo strain, we aimed to achieve the same in C1-G-S-Aux. For this purpose, we refactored the C1–S-Evo strain, instead of introducing the necessary mutations in C1-G-S-Aux. We deleted the *ltaE* and *aceA* genes to prevent glycine formation and reintroduced the C2 module in the genome. This strain, termed C1-G-S-Evo, was transformed with pC1 and the mutated pCO_2, and growth was assessed on 20 mM glucose and 50% CO_2. The strain expressing all three modules was able to sustain growth, albeit very slowly and with a low biomass yield (Fig. S6). Although promising, further optimizations are needed to build toward strains that can generate all biomass from CO_2 via the thermodynamically challenging reduction by FDH.

3. Discussion

In this study, we successfully laid the foundation for synthetic C1-metabolism in the industrial workhorse *P. putida*. We were able to demonstrate formate, methanol, and CO_2 assimilation through heterologous expression of the core modules of the rGlyP in growth-coupled, auxotrophic selection strains. We show functional expression of all key modules of the rGlyP until serine using both formate and methanol as substrate. The demonstrated conversion in C1-G-S-Aux of methanol and formate into glycine and serine (together forming ~11% of cellular biomass (Claassens et al., 2019a,b)) provides a strong basis for full formatotrophy and methylotrophy in *P. putida*. Full C1-dependent growth on both substrates can likely be achieved by a combination of genomic integration and further fine-tuning of the enzymes of the independent modules. Then, a combination of rational engineering and adaptive laboratory evolution can be used to optimize the complete metabolic network. This approach has been shown to be efficient in establishing full formatotrophy in both *E. coli* and *C. necator* (Claassens et al., 2020; Dronsella et al., 2022; Kim et al., 2020). Recently, the first proof of concept of bioproduction has been established with a synthetic formatotrophic *E.coli* (Kim et al., 2022). Here they further optimized the bacterium through adaptive laboratory evolution and were able to produce lactate from formate at 10% of the theoretical maximum. The establishment of full C1-dependent growth in *P. putida* will also open many avenues for C1-based industrial biotechnology, given the many attractive properties, and demonstrated production pathways available for this bacterium.

Establishing full formatotrophy in *P. putida* can benefit from its native catalytically fast, metal-dependent FDH, to provide energy to run the rGlyP. So far, full formatotrophic growth in *E. coli* was only demonstrated by heterologously expressing a kinetically slower non-metal-dependent FDH, likely limiting formatotrophic growth rates (Bar-Even et al., 2013; Gleizer et al., 2019; Kim et al., 2020). In parallel with this study, Turlin et al., (2022) demonstrated formate assimilation in *P. putida* into most of its biomass via the full rGlyP, while acetate supplies energy and a small fraction of biomass. However, as *P. putida* contains a kinetically fast FDH, further evolution can potentially replace acetate with formate as the sole energy source, establishing full formatotrophic growth. Moreover, once equipped with the M or CO_2 module presented in this study, this future strain could be further evolved towards full methylotrophy or chemolithoautotrophy.

In this work, we showcase a specific promising feature to engineer methanol conversion in *P. putida*, by demonstrating methanol-dependent growth through PQQ-dependent MDH activity. Methanol oxidation is frequently pinpointed as the major bottleneck during the ongoing efforts to establish synthetic methylotrophy in other organisms (Antoniewicz, 2019; Wang et al., 2020). The NAD-dependent enzymes can lead to higher biomass yields but come with disadvantageous thermodynamics. The PQQ-dependent enzymes do cause a slight reduction in biomass yield, but their higher thermodynamics could lead to higher growth rates (Claassens et al., 2022; Cotton et al., 2020; Whitaker et al., 2015). So far, none of the published metabolic engineering efforts toward synthetic methylotrophy has demonstrated the engineered expression of a PQQ-dependent MDH.

As we demonstrate here, *P. putida* is a promising host to relatively easily establish PQQ-dependent synthetic methylotrophy, due to its native PQQ biosynthesis and PQQ-alcohol dehydrogenase that could execute PQQ-MDH activity (Wehrmann et al., 2017). So, it will be easier to establish PQQ-dependent methylotrophy in *P. putida* than in for example *E. coli*, which natively lacks PQQ-biosynthesis (Yang et al., 2010). Although methanol-dependent growth in C1–S-Aux via PQQ-MDH is slower than via the NADH-MDH, these results establish the basis to further develop this industrially attractive phenotype. The native PQQ-MDH candidate enzyme used in this study could be further engineered through directed evolution toward higher specificity and activity on methanol. In summary, both NAD-and PQQ-dependent MDHs could be further explored to realize efficient and fast synthetic methylotrophy in *P. putida*.

This study shows engineered CO_2 fixation via the reverse activity of FDH. In recent years, CO_2 to formate reduction has been proposed for sustainable biotechnology as a promising feature for both engineered *in vitro* and *in vivo* CO_2 fixation. However, so far experimental evidence of engineered CO_2 fixation via FDH has only been shown for *in vitro* CO_2 reduction. These *in vitro* studies were based on metal-dependent FDH enzymes, from for example *C. necator* and *Rhodobacter capsulatus* (Hartmann and Leimkühler, 2013; X. Yu et al., 2017). The high *in vitro* catalytic rates found for CO_2 reduction to formate of these metal-dependent FDH enzymes (as opposed to slower non-metal-dependent FDHs) are a promising indication that engineered *in vivo* synthetic CO_2 fixation via metal-dependent FDH is achievable. However, engineered *in vivo* activity from CO_2 to formate by a metal-dependent FDH was not shown yet, possibly due to the complexity of overexpressing metal-dependent FDHs, which typically require chaperones and consist of multiple subunits. In addition, the reduction of CO_2 to formate by FDH is thermodynamically relatively challenging, likely requiring a very high substrate (CO_2 and NADH) to product (formate and NAD^+) ratio within the cell.

We overcome these limitations by expressing the native metal-dependent FDH at elevated CO_2 levels, enabling FDH-mediated CO_2 reduction activity *in vivo*. By using a growth-coupled selection strategy, we show that the reaction can carry sufficient flux to supply the cell with the C1-precursors and the beta-carbon of serine (forming ~4% of cellular biomass) (Claassens et al., 2019a,b). However, this growth phenotype required short-term laboratory evolution, which resulted in fine-tuning of FDH expression and an essential early stop codon mutation in the NuoG subunit of complex I in the electron transport chain. This likely increased the $NADH/NAD^+$ ratio, facilitating the thermodynamics of CO_2 reduction to formate. In *E. coli*, it has been shown that a similar deletion rendered complex I non-functional, most likely resulting in an unbalanced NADH/NAD + ratio (Falk-Krzesinski and Wolfe, 1998). This indicates that the establishment of CO_2 fixation via FDH in *P. putida* and potentially other organisms require modulation of the $NADH/NAD^+$ ratio. Alternatively, metal-dependent NADPH-FDHs could be further developed for CO_2 reduction, as cells typically maintain a higher $NADPH/NADP^+$ ratio compared to $NADH/NAD^+$ (Calzadiaz-Ramirez and Meyer, 2022).

Demonstrating efficient CO_2 reduction until serine in the C1-G-S-auxotroph was still not achieved. This likely reflects the more challenging redox requirements to realize this higher flux towards all C1-precursors, glycine, and serine in the cell. The reduction of CO_2 to formate could probably be further improved by redox-factor engineering approaches mentioned above and possibly with further expression and maturation optimization of FDH or other engineered or heterologous metal-dependent FDH candidates, which could be potentially even faster.

Overall, achieving growth with CO_2 as the sole carbon source (synthetic autotrophy) in *P. putida* via the rGlyP would be a very promising feature for sustainable industrial biotechnology. This would also require a suitable inorganic electron donor, for which hydrogen is an interesting candidate as it can be produced very efficiently from renewable electricity (Claassens et al., 2018). The soluble oxygen-tolerant NAD-reducing hydrogenase from *C. necator* has already been successfully expressed *in vivo* in *P. putida* as an NADH regeneration system for product synthesis (Lonsdale et al., 2015). This NADH regeneration system combined with the here established CO_2 reduction could enable synthetic autotrophy in *P. putida* based on the rGlyP. If the FDH activity could be increased, which based on *in vitro* data could be faster than Rubisco (Cotton et al., 2018), the rGlyP could possibly be a kinetically faster alternative to the naturally, ubiquitous Calvin cycle. This, together with the lower ATP costs of the rGlyP versus the Calvin Cycle makes it an attractive pathway to explore for synthetic autotrophy in *P. putida* and other organisms.

Overall, this work widens the possibilities for engineered C1-assimilation based on the versatile rGlyP and shows the suitability of *P. putida* for C1-based biotechnology through lifestyle engineering. The successful establishment of synthetic C1-assimilation in *P. putida* is a key step towards its usefulness in contributing to realize a truly sustainable C1-based biotechnology.

4. Methods

4.1. Plasmids, primers, and strains

All strains and plasmids used in the present study are listed in Table S1 and S2. Primers used for plasmid construction and gene deletions are listed in Table S3.

4.2. Bacterial strains and growth conditions

P. putida and *E. coli* cultures were incubated at 30 °C and 37 °C respectively. For cloning purposes, both strains were propagated in Lysogeny Broth (LB) medium containing 10 g/L NaCl, 10 g/L tryptone, and 5 g/L yeast extract. For the preparation of solid media, 1.5% (w/v) agar was added. Antibiotics, when required, were used at the following concentrations: kanamycin (Km) 50 μg/ml, gentamycin (Gm) 10 μg/ml, chloramphenicol (Cm) 50 μg/ml and apramycin (Apra) 50 μg/ml. All growth experiments were performed using M9 minimal medium (per Liter; 3.88 g K_2HPO_4, 1.63 g NaH_2PO_4, 2.0 g $(NH_4)_2SO_4$, pH 7.0. The M9 media was supplemented with a trace elements solution (per Liter; 10 mg/L ethylenediaminetetraacetic acid (EDTA), 0.1 g/L $MgCl_2.6H_2O$ 2 mg/L $ZnSO_4•7H_2O$, 1 mg/L$CaCl_2•2H_2O$, 5 mg/L$FeSO_4•7H_2O$, 0.2 mg/L, $Na_2MoO_4•2H_2O$, 0.2 mg/L $CuSO_4•5H_2O$, 0.4 mg/L $CoCl_2•6H_2O$, 1 mg/L $MnCl_2•2H_2O$). Before the growth experiments, cells were pre-grown in non-selective M9 media, containing 10 mM glucose and 2 mM serine, before being transferred to selective growth conditions. In all growth experiments, precultured strains were washed twice in M9 media without a carbon source before transfer and inoculated at an OD_{600} of 0.1. Selective growth conditions consisted of unless otherwise indicated, 10 mM glucose +5 mM glycine (C1–S-Aux) or 10 mM glucose (C1-G-S-Aux) supplemented with relevant C1-substrates (30 mM formate or 500 mM methanol or 50% (v/v) CO_2). For the formate and methanol experiments with C1-G-S-Aux, 100 mM sodium bicarbonate was added to the medium to push the GCS in the reverse direction. Upon addition of sodium bicarbonate, the pH was readjusted to 7.0 with 1M HCl. Plate reader experiments were carried out in 200 μL of M9 medium using a Synergy plate reader (Biotek). Growth (OD_{600}) was measured over time using continuous linear shaking (567 cpm, 3 mm) and measurements were taken every 5 min. Plates were covered with a Breath-Easy® sealing membrane (Sigma-Aldrich). For the CO_2-dependent growth experiments, 100 mL glass bottles were filled for 10% (10 mL) with liquid M9 media. Subsequently, the headspace (90%) was filled with the desired CO_2 concentration before autoclavation. Carbon sources and antibiotics were added after sterilization and cultures were incubated in a rotary shaker at 200 rpm at 30 °C. All growth experiments were performed in biological triplicates and the represented growth curves show the average of these triplicates.

4.3. Plasmid construction

Plasmids were constructed using the standard protocols of the previously described SevaBrick Assembly (Damalas et al., 2020). All DNA fragments were amplified using Q5® Hot Start High-Fidelity DNA Polymerase (New England Biolabs). To construct the C1 module, DNA fragments of the *fhs*, *fchA,* and *folD* genes from *Clostridium ljunghdahlli* DSM13528 were codon-optimized with the JCat tool (Grote et al., 2005) and synthesized through Genescript. The MDH genes from *Geobacillus. stearothermophilus, Bacillus. methanolicus, Corynebacterium glutamicum,* and an engineered variant from *Cupriavidus necator* (Wu et al., 2016) were codon-optimized and synthesized by IDT (Integrated DNA Technologies) (Table S5). All genes in this study were expressed under the control of a strong constitutive promoter (BBa_J23100) and RBS (BBa_B0034). All plasmids were transformed using heat shock in chemically competent *E. coli* DH5α λpir and selected on LB agar with corresponding antibiotics. Colonies were screened through colony PCR with Phire Hot Start II DNA Polymerase (Thermo Fisher Scientific). Isolated plasmids were verified using Sanger sequencing (MACROGEN inc.) and subsequently transformed into *P. putida* via electroporation.

4.4. Genome modification

Genomic deletions in this study were performed using the protocol previously described by Wirth et al. (2020). Homology regions of ±500 bp were amplified up and downstream of the target gene from the genome of *P. putida* KT2440. Both regions were cloned into the non-replicative pGNW vector and propagated in *E. coli* DH5α λpir. Correct plasmids were transformed into *P. putida* by electroporation and selected on LB + Km plates. Successful co-integrations were verified by PCR. Hereafter, co-integrated strains were transformed with the pQURE6-H, and transformants were plated on LB + Gm containing 2 mM 3- methylbenzoic acid (3-mBz). This compound induces the XylS-dependent Pm promoter, regulating the *I-Sce*I homing nuclease that cuts the integrated pGNW vector. Successful gene deletions were verified by PCR and Sanger sequencing (MACROGEN inc). Hereafter, the pQURE6-H was cured by removing the selective pressure and its loss was verified by sensitivity to gentamycin.

4.5. Promoter characterization

P. putida strains expressing GFP under the normal or mutated J23100 promoter or containing an empty vector were grown in biological triplicates in M9 medium +10 mM glucose. Cell density (OD600) and GFP fluorescence (excitation 485 nm, emission 512 nm, gain 50) were measured using a Synergy plate reader (Biotek) over time using continuous linear shaking, and measurements were taken every 5 min. The promoter strength was quantified based on fluorescence normalized per cell density (RFU/OD600) after 20 h of cultivation when cells had reached the stationary phase. Values were corrected for background fluorescence of cells without GFP.

4.6. Whole-genome sequencing

Genomic DNA of the evolved mutants and the unevolved parent strain was isolated from LB overnight cultures using the GenElute™ Bacterial Genomic DNA Kit (Sigma-Aldrich St. Louis, MO). The extracted DNA was evaluated by gel electrophoresis and quantified by a NanoDrop spectrophotometer (Thermo Fisher Scientific). Samples were sent for Illumina sequencing to Novogene Co. Ltd. (Beijing, China). Raw Illumina reads were trimmed for low quality and adapters with fastp (v0.20.0). Mutations were identified by comparing the reads to the annotated reference genome of *Pseudomonas putida* KT2440 (GCF_000007565.2) using breseq (v0.35.5) (Barrick et al., 2014).

4.7. Carbon labeling

For stationary isotope tracing of the proteinogenic amino acids, cultures were grown in 10 ml of M9 media under the previously described experimental conditions. Media was composed of unlabeled (glucose and glycine) and labeled (formate-^{13}C, methanol-^{13}C, and $^{13}CO_2$) (Sigma, 99 atom %) carbon sources. Cells were cultivated in two successive cultures with labeled or unlabeled carbon to diminish the labeling effects of the preculture. Hereafter, the approximate cell volume was harvested that has the cellular biomass roughly equivalent to 1 mL with an OD600 of 1 was taken and pelleted down. The pellet was washed with 1 mL of pure water and pelleted down again. The pellet was resuspended in 1 ml of 6N HCl and incubated for 24 h at 95 °C. Then, the caps were opened, allowing evaporation under continuous airflow. The resulting pellet was resuspended in 1 mL of pure water and centrifugated for 5 min at full speed to remove residual particles. The hydrolysate was analyzed using ultra-performance liquid chromatography (UPLC) (Acquity, Waters) using an HSS T3 C18-reversed-phase column (Waters). The mobile phases were 0.1% formic acid in H_2O (A) and 0.1% formic acid in acetonitrile (B). The flow rate was 400 μL/min and the following gradient was used: 0–1 min 99% A; 1–5 min gradient from 99% A to 82%; 5–6 min gradient from 82% A to 1% A; 6–8 min 1% A; 8–8.5 min gradient to 99% A; 8.5–11 min-re-equilibrate with 99% A. Mass spectra were acquired using an Exactive mass spectrometer (MS) (Thermo Scientific) in positive ionization mode. Data analysis was performed using Xcalibur (Thermo Scientific). The identification of amino acids was based on retention times and m/z values obtained from amino acid standards (Sigma-Aldrich)

Author statement

We thank all reviewers for their critical analyses and suggestions, all of which helped us improving the manuscript considerably. We provide hereby the point-by-point rebuttal, having addressed as well as we could the concerns by the reviewers. We hope this work can be subsequently accepted for publication.

Declaration of competing interest

The authors declare no conflict of interest.

Data availability

Data will be made available on request.

Acknowledgments

We are grateful to Iame Alves Guedes and Sara Cantera Ruiz de Pellon for their invaluable help with the CO_2-dependent experiments. We thank Bart Nijse for the analysis of the whole genome sequencing. This work was financed by the European Union's Horizon2020 Research and Innovation Program under grant agreement Nos. 635536 (EmPowerPutida) 730976 (IBISBA) and 101070281 (BIOS) to V.A.P.M. d.S.

Appendix A. Supplementary data

Supplementary data to this article can be found online at https://doi.org/10.1016/j.ymben.2023.02.004.

References

Ankenbauer, A., Schäfer, R.A., Viegas, S.C., Pobre, V., Voß, B., Arraiano, C.M., Takors, R., 2020. Pseudomonas putida KT2440 is naturally endowed to withstand industrial-scale stress conditions. Microb. Biotechnol. 13 (4), 1145–1161. https://doi.org/10.1111/1751-7915.13571.

Antoniewicz, M.R., 2019. Synthetic methylotrophy: strategies to assimilate methanol for growth and chemicals production. Curr. Opin. Biotechnol. 59, 165–174. https://doi.org/10.1016/j.copbio.2019.07.001.

Bar-Even, A., Noor, E., Flamholz, A., Milo, R., 2013. Design and analysis of metabolic pathways supporting formatotrophic growth for electricity-dependent cultivation of microbes. Biochim. Biophys. Acta Bioenerg. 1827 (8–9), 1039–1047. https://doi.org/10.1016/j.bbabio.2012.10.013.

Barenholz, U., Davidi, D., Reznik, E., Bar-On, Y., Antonovsky, N., Noor, E., Milo, R., 2017. Design principles of autocatalytic cycles constrain enzyme kinetics and force low substrate saturation at flux branch points. Elife 6, 1–32. https://doi.org/10.7554/elife.20667.

Barrick, J.E., Colburn, G., Deatherage, D.E., Traverse, C.C., Strand, M.D., Borges, J.J., Knoester, D.B., Reba, A., Meyer, A.G., 2014. Identifying structural variation in haploid microbial genomes from short-read resequencing data using breseq. BMC Genom. 15 (1), 1–17. https://doi.org/10.1186/1471-2164-15-1039.

Bertsch, J., Müller, V., 2015. Bioenergetic constraints for conversion of syngas to biofuels in acetogenic bacteria. Biotechnol. Biofuels 8 (1), 1–12. https://doi.org/10.1186/s13068-015-0393-x.

Calzadiaz-Ramirez, L., Meyer, A.S., 2022. Formate dehydrogenases for CO2 utilization. Curr. Opin. Biotechnol. 73, 95–100. https://doi.org/10.1016/j.copbio.2021.07.011.

Chadwick, G.L., Hemp, J., Fischer, W.W., Orphan, V.J., 2018. Convergent evolution of unusual complex I homologs with increased proton pumping capacity: energetic and ecological implications. ISME J. 12 (11), 2668–2680. https://doi.org/10.1038/s41396-018-0210-1.

Chen, F.Y.H., Jung, H.W., Tsuei, C.Y., Liao, J.C., 2020. Converting Escherichia coli to a synthetic methylotroph growing solely on methanol. Cell 182 (4), 933–946.e14. https://doi.org/10.1016/j.cell.2020.07.010.

Choe, H., Joo, J.C., Cho, D.H., Kim, M.H., Lee, S.H., Jung, K.D., Kim, Y.H., 2014. Efficient CO2-reducing activity of NAD-dependent formate dehydrogenase from Thiobacillus sp. KNK65MA for formate production from CO 2 gas. PLoS One 9 (7), 14–16. https://doi.org/10.1371/journal.pone.0103111.

Claassens, Nico J., Bordanaba-Florit, G., Cotton, C.A.R., De Maria, A., Finger-Bou, M., Friedeheim, L., Giner-Laguarda, N., Munar-Palmer, M., Newell, W., Scarinci, G., Verbunt, J., de Vries, S.T., Yilmaz, S., Bar-Even, A., 2020. Replacing the Calvin cycle with the reductive glycine pathway in Cupriavidus necator. Metab. Eng. 62, 30–41. https://doi.org/10.1016/j.ymben.2020.08.004.

Claassens, Nico J., Cotton, C.A.R., Kopljar, D., Bar-Even, A., 2019a. Making quantitative sense of electromicrobial production. Nature Catalys. 2 (5), 437–447. https://doi.org/10.1038/s41929-019-0272-0.

Claassens, Nico J., He, H., Bar-Even, A., 2019b. Synthetic methanol and formate assimilation via modular engineering and selection strategies. Methylotrophs and Methylotroph Communities 5. https://doi.org/10.21775/9781912530045.14.

Claassens, Nico J., Satanowski, A., Bysani, V.R., Dronsella, B., Orsi, E., Rainaldi, V., Yilmaz, S., Wenk, S., Lindner, S.N., 2022. Engineering the Reductive Glycine Pathway: A Promising Synthetic Metabolism Approach for C1-Assimilation.

Claassens, Joannes, Nico, Sánchez-Andrea, I., Sousa, D.Z., Bar-Even, A., 2018. Towards sustainable feedstocks: a guide to electron donors for microbial carbon fixation. Curr. Opin. Biotechnol. 50 (ii), 195–205. https://doi.org/10.1016/j.copbio.2018.01.019.

Cotton, C.A., Claassens, N.J., Benito-Vaquerizo, S., Bar-Even, A., 2020. Renewable methanol and formate as microbial feedstocks. Curr. Opin. Biotechnol. 62, 168–180. https://doi.org/10.1016/j.copbio.2019.10.002.

Cotton, C.A., Edlich-Muth, C., Bar-Even, A., 2018. Reinforcing carbon fixation: CO2 reduction replacing and supporting carboxylation. Curr. Opin. Biotechnol. 49, 49–56. https://doi.org/10.1016/j.copbio.2017.07.014.

Damalas, S.G., Batianis, C., Martin-Pascual, M., de Lorenzo, V., Martins dos Santos, V.A. P., 2020. Seva 3.1: enabling interoperability of DNA assembly among the SEVA, BioBricks and Type IIS restriction enzyme standards. Microb. Biotechnol. 13 (6), 1793–1806. https://doi.org/10.1111/1751-7915.13609.

Dronsella, B., Orsi, E., Benito-vaquerizo, S., Glatter, T., Bar-even, A., Claassens, N.J., 2022. Engineered synthetic one-carbon fixation exceeds yield of the Calvin Cycle. bioRxiv. https://doi.org/10.1101/2022.10.19.512895 bioRxiv preprint doi.

Falk-Krzesinski, H.J., Wolfe, A.J., 1998. Genetic analysis of the nuo locus, which encodes the proton- translocating NADH dehydrogenase in Escherichia coli. J. Bacteriol. 180 (5), 1174–1184. https://doi.org/10.1128/jb.180.5.1174-1184.1998.

Fan, L., Xia, C., Zhu, P., Lu, Y., Wang, H., 2020. Electrochemical CO2 reduction to high-concentration pure formic acid solutions in an all-solid-state reactor. Nat. Commun. 11 (1), 1–9. https://doi.org/10.1038/s41467-020-17403-1.

Figueroa, I.A., Barnum, T.P., Somasekhar, P.Y., Carlström, C.I., Engelbrektson, A.L., Coates, J.D., 2018. Metagenomics-guided analysis of microbial

chemolithoautotrophic phosphite oxidation yields evidence of a seventh natural CO2 fixation pathway. Proc. Natl. Acad. Sci. U.S.A. 115 (1), E92–E101. https://doi.org/10.1073/pnas.1715549114.

Flamholz, A., Noor, E., Bar-Even, A., Milo, R., 2012. EQuilibrator - the biochemical thermodynamics calculator. Nucleic Acids Res. 40 (D1) https://doi.org/10.1093/nar/gkr874.

Gleizer, S., Ben-Nissan, R., Bar-On, Y.M., Antonovsky, N., Noor, E., Zohar, Y., Jona, G., Krieger, E., Shamshoum, M., Bar-Even, A., Milo, R., 2019. Conversion of Escherichia coli to generate all biomass carbon from CO2. Cell 179 (6), 1255–1263.e12. https://doi.org/10.1016/j.cell.2019.11.009.

Gonzalez De La Cruz, J., Machens, F., Messerschmidt, K., Bar-Even, A., 2019. Core catalysis of the reductive Glycine pathway demonstrated in yeast. ACS Synth. Biol. 8 (5), 911–917. https://doi.org/10.1021/acssynbio.8b00464.

Grote, A., Hiller, K., Scheer, M., Münch, R., Nörtemann, B., Hempel, D.C., Jahn, D., 2005. JCat: a novel tool to adapt codon usage of a target gene to its potential expression host. Nucleic Acids Res. 33 (Suppl. 2), 526–531. https://doi.org/10.1093/nar/gki376.

Hartmann, T., Leimkühler, S., 2013. The oxygen-tolerant and NAD+-dependent formate dehydrogenase from Rhodobacter capsulatus is able to catalyze the reduction of CO2 to formate. FEBS J. 280 (23), 6083–6096. https://doi.org/10.1111/febs.12528.

Keller, P., Reiter, M.A., Kiefer, P., Gassler, T., Hemmerle, L., Christen, P., Noor, E., Vorholt, J.A., 2022. Generation of an Escherichia coli strain growing on methanol via the ribulose monophosphate cycle. Nat. Commun. 13 (1), 1–13. https://doi.org/10.1038/s41467-022-32744-9.

Kim, S., David Giraldo, N., Rainaldi, V., Machens, F., Collas, F., Kensy, F., Bar-Even, A., Lindner, S.N., 2022. Optimizing E. coli as a Formatotrophic Platform for Bioproduction via the 1 Reductive glycine Pathway 2. https://doi.org/10.1101/2022.08.23.504942.

Kim, S., Lindner, S.N., Aslan, S., Yishai, O., Wenk, S., Schann, K., Bar-Even, A., 2020. Growth of E. coli on formate and methanol via the reductive glycine pathway. Nat. Chem. Biol. 16 (5), 538–545. https://doi.org/10.1038/s41589-020-0473-5.

Koopman, F.W., De Winde, J.H., Ruijssenaars, H.J., 2009. C1 compounds as auxiliary substrate for engineered Pseudomonas putida S12. Appl. Microbiol. Biotechnol. 83 (4), 705–713. https://doi.org/10.1007/s00253-009-1922-y.

Köpke, M., Simpson, S.D., 2020. Pollution to products: recycling of 'above ground' carbon by gas fermentation. Curr. Opin. Biotechnol. 65, 180–189. https://doi.org/10.1016/j.copbio.2020.02.017.

Liew, F.E., Nogle, R., Abdalla, T., Rasor, B.J., Canter, C., Jensen, R.O., Wang, L., Strutz, J., Chirania, P., De Tissera, S., Mueller, A.P., Ruan, Z., Gao, A., Tran, L., Engle, N.L., Bromley, J.C., Daniell, J., Conrado, R., Tschaplinski, T.J., et al., 2022. Carbon-negative production of acetone and isopropanol by gas fermentation at industrial pilot scale. Nat. Biotechnol. 40 (3), 335–344. https://doi.org/10.1038/s41587-021-01195-w.

Liu, Z., Wang, K., Chen, Y., Tan, T., Nielsen, J., 2020. Third-generation biorefineries as the means to produce fuels and chemicals from CO2. Nature Catalys. 3 (3), 274–288. https://doi.org/10.1038/s41929-019-0421-5.

Lonsdale, T.H., Lauterbach, L., Honda Malca, S., Nestl, B.M., Hauer, B., Lenz, O., 2015. H2-driven biotransformation of n-octane to 1-octanol by a recombinant Pseudomonas putida strain co-synthesizing an O2-tolerant hydrogenase and a P450 monooxygenase. Chem. Commun. 51 (90), 16173–16175. https://doi.org/10.1039/c5cc06078h.

Löwe, H., Kremling, A., 2021. Depth computational analysis of natural and artificial carbon fixation pathways. BioDesign Research 2021 (i). https://doi.org/10.34133/2021/9898316.

Maia, L.B., Moura, I., Moura, J.J.G., 2017. Molybdenum and tungsten-containing formate dehydrogenases: aiming to inspire a catalyst for carbon dioxide utilization. Inorg. Chim. Acta. 455, 350–363. https://doi.org/10.1016/j.ica.2016.07.010.

Martin-Pascual, M., Batianis, C., Bruinsma, L., Asin-Garcia, E., Garcia-Morales, L., Weusthuis, R.A., van Kranenburg, R., Martins dos Santos, V.A.P., 2021. A navigation guide of synthetic biology tools for Pseudomonas putida. Biotechnol. Adv. 49 (March), 107732 https://doi.org/10.1016/j.biotechadv.2021.107732.

Naik, S.N., Goud, V.V., Rout, P.K., Dalai, A.K., 2010. Production of first and second generation biofuels: a comprehensive review. Renew. Sustain. Energy Rev. 14 (2), 578–597. https://doi.org/10.1016/j.rser.2009.10.003.

Nies, S.C., Dinger, R., Chen, Y., Wordofa, G.G., Kristensen, M., Schneider, K., Petzold, C. J., Keasling, J.D., Blank, L.M., Ebert, B.E., 2020. Crossm Systems Analysis of NADH Dehydrogenase Mutants Reveals, vol. 86, pp. 1–17, 11.

Nikel, P.I., de Lorenzo, V., 2018. Pseudomonas putida as a functional chassis for industrial biocatalysis: from native biochemistry to trans-metabolism. Metab. Eng. 50 (April), 142–155. https://doi.org/10.1016/j.ymben.2018.05.005.

Orsi, E., Claassens, N.J., Nikel, P.I., Lindner, S.N., 2021. Growth-coupled selection of synthetic modules to accelerate cell factory development. Nat. Commun. 12 (1), 1–5. https://doi.org/10.1038/s41467-021-25665-6.

Poblete-Castro, I., Becker, J., Dohnt, K., Santos, V. M. Dos, Wittmann, C., 2012. Industrial biotechnology of Pseudomonas putida and related species. Appl. Microbiol. Biotechnol. 93 (6), 2279–2290. https://doi.org/10.1007/s00253-012-3928-0.

Ragsdale, S.W., Wood, H.G., 1991. Enzymology of the acetyl-coa pathway of CO2 fixation. Crit. Rev. Biochem. Mol. Biol. 26 (3–4), 261–300. https://doi.org/10.3109/10409239109114070.

Reda, T., Plugge, C.M., Abram, N.J., Hirst, J., 2008. Reversible interconversion of carbon dioxide and formate by an electroactive enzyme. Proc. Natl. Acad. Sci. U.S.A. 105 (31), 10654–10658. https://doi.org/10.1073/pnas.0801290105.

Sánchez-Andrea, I., Guedes, I.A., Hornung, B., Boeren, S., Lawson, C.E., Sousa, D.Z., Bar-Even, A., Claassens, N.J., Stams, A.J.M., 2020. The reductive glycine pathway allows autotrophic growth of Desulfovibrio desulfuricans. Nat. Commun. 11 (1), 1–12. https://doi.org/10.1038/s41467-020-18906-7.

Stöckl, M., Claassens, N.J., Lindner, S.N., Klemm, E., Holtmann, D., 2022. Coupling electrochemical CO2 reduction to microbial product generation – identification of the gaps and opportunities. Curr. Opin. Biotechnol. 74, 154–163. https://doi.org/10.1016/j.copbio.2021.11.007.

Szima, S., Cormos, C.C., 2018. Improving methanol synthesis from carbon-free H2 and captured CO2: a techno-economic and environmental evaluation. J. CO2 Util. 24 (March), 555–563. https://doi.org/10.1016/j.jcou.2018.02.007.

Turlin, J., Dronsella, B., Maria, A. De, Lindner, S.N., Nikel, P.I., 2022. Integrated rational and evolutionary engineering of genome-reduced Pseudomonas putida strains empowers synthetic formate assimilation. Metab. Eng. 74 (November), 2022. https://doi.org/10.1016/j.ymben.2022.10.008, 07.10.499488.

Wang, Y., Fan, L., Tuyishime, P., Zheng, P., Sun, J., 2020. Synthetic methylotrophy: a practical solution for methanol-based biomanufacturing. Trends Biotechnol. 38 (6), 650–666. https://doi.org/10.1016/j.tibtech.2019.12.013.

Wehrmann, M., Billard, P., Martin-Meriadac, A., Zegeye, A., Klebensberger, J., 2017. Crossm Functional Role of Lanthanides in Enzymatic Activity and Transcriptional Regulation of Pyrroloquinoline Quinone- Dependent Alcohol Dehydrogenases in.

Wendisch, V.F., Brito, L.F., Gil Lopez, M., Hennig, G., Pfeifenschneider, J., Sgobba, E., Veldmann, K.H., 2016. The flexible feedstock concept in Industrial Biotechnology: metabolic engineering of Escherichia coli, Corynebacterium glutamicum, Pseudomonas, Bacillus and yeast strains for access to alternative carbon sources. J. Biotechnol. 234, 139–157. https://doi.org/10.1016/j.jbiotec.2016.07.022.

Wenk, S., Schann, K., He, H., Rainaldi, V., Kim, S., Lindner, S.N., Bar-Even, A., 2020. An "energy-auxotroph" Escherichia coli provides an in vivo platform for assessing NADH regeneration systems. Biotechnol. Bioeng. 117 (11), 3422–3434. https://doi.org/10.1002/bit.27490.

Whitaker, W.B., Sandoval, N.R., Bennett, R.K., Fast, A.G., Papoutsakis, E.T., 2015. Synthetic methylotrophy: engineering the production of biofuels and chemicals based on the biology of aerobic methanol utilization. Curr. Opin. Biotechnol. 33, 165–175. https://doi.org/10.1016/j.copbio.2015.01.007.

Wirth, N.T., Kozaeva, E., Nikel, P.I., 2020. Accelerated genome engineering of Pseudomonas putida by I-SceI–mediated recombination and CRISPR-Cas9 counterselection. Microb. Biotechnol. 13 (1), 233–249. https://doi.org/10.1111/1751-7915.13396.

Woolston, B.M., King, J.R., Reiter, M., Van Hove, B., Stephanopoulos, G., 2018. Improving formaldehyde consumption drives methanol assimilation in engineered E. coli. Nat. Commun. 9 (1) https://doi.org/10.1038/s41467-018-04795-4.

Wu, T.Y., Chen, C.T., Liu, J.T.J., Bogorad, I.W., Damoiseaux, R., Liao, J.C., 2016. Characterization and evolution of an activator-independent methanol dehydrogenase from Cupriavidus necator N-1. Appl. Microbiol. Biotechnol. 100 (11), 4969–4983. https://doi.org/10.1007/s00253-016-7320-3.

Yang, X.P., Zhong, G.F., Lin, J.P., Mao, D. Bin, Wei, D.Z., 2010. Pyrroloquinoline quinone biosynthesis in Escherichia coli through expression of the Gluconobacter oxydans pqqABCDE gene cluster. J. Ind. Microbiol. Biotechnol. 37 (6), 575–580. https://doi.org/10.1007/s10295-010-0703-z.

Yishai, O., Bouzon, M., Döring, V., Bar-Even, A., 2018. In vivo assimilation of one-carbon via a synthetic reductive Glycine pathway in Escherichia coli. ACS Synth. Biol. 7 (9), 2023–2028. https://doi.org/10.1021/acssynbio.8b00131.

Yishai, O., Goldbach, L., Tenenboim, H., Lindner, S.N., Bar-Even, A., 2017. Engineered assimilation of exogenous and endogenous formate in Escherichia coli. ACS Synth. Biol. 6 (9), 1722–1731. https://doi.org/10.1021/acssynbio.7b00086.

Yu, H., Liao, J.C., 2018. A modified serine cycle in Escherichia coli coverts methanol and CO2 to two-carbon compounds. Nat. Commun. 9 (1) https://doi.org/10.1038/s41467-018-06496-4.

Yu, X., Niks, D., Mulchandani, A., Hille, R., 2017. Efficient reduction of CO2 by the molybdenum-containing formate dehydrogenase from Cupriavidus necator (Ralstonia eutropha). J. Biol. Chem. 292 (41), 16872–16879. https://doi.org/10.1074/jbc.M117.785576.

Zobel, S., Kuepper, J., Ebert, B., Wierckx, N., Blank, L.M., 2017. Metabolic response of Pseudomonas putida to increased NADH regeneration rates. Eng. Life Sci. 17 (1), 47–57. https://doi.org/10.1002/elsc.201600072.